CORRECTION OF STRUCTURED NOISE IN FMRI USING SPATIAL INDEPENDENT COMPONENT ANALYSIS : CORSICA

Vincent Perlbarg[1]*, Pierre Bellec*[1]*, Jean-Luc Anton*[2]*, Habib Benali*[1]

[1]INSERM U678-UPMC, Paris, France
[2]Centre IRMf, CHU Hôpital de la Timone, Marseille, France

ABSTRACT

The physiological fluctuations (breathing and heartbeat) and brain movements are the main sources of confounds in activation and functional connectivity studies in functional magnetic resonance imaging (fMRI). The main difficulty to cope with these effects is the aliasing of cardiac and possible respiration signals for acquisitions with long TR (typically TR $>$ 1s). We proposed a method of structured noise correction based on spatial Independent Component Analysis, able to extract components linked to cardio-respiratory activity and brain movements. The automatic selection of noise-related components was based on a stepwise regression procedure using "true" physiological noise time courses as reference (extracted from regions of interest in the cerebro-spinal fluid and near major blood vessels). We evaluated the sensitivity of the selection on long-TR and short-TR datasets and we showed that our method was efficient even for long-TR datasets.

1. INTRODUCTION

Functional magnetic resonance imaging (fMRI) is a noninvasive technique for mapping brain activity through the blood oxygenation level dependent (BOLD) effect. BOLD signal depends on blood oxygenation, blood flow and blood volume variations due to neural hemodynamics. The major fluctuations of no-interest that corrupt the BOLD signal include rapid and slow head movements and physiological activity (breathing and heartbeat). On the one hand, these fluctuations induce an increase data variance and thereby decrease the sensitivity of activity detection. On the other hand, these temporally correlated fluctuations are a critical sources of confounds in functional connectivity studies in fMRI.

The effects due to respiration and heartbeat in fMRI have been described and are quite different. Respiration induces firstly small variations in the static magnetic field [1] and secondly, movements of the chest induce global movements of the head at the respiratory frequency preponderant in the cerebro-spinal fluid (CSF) pools such as the ventricles or the outline of the brain [2]. Heartbeat induces variations of blood flow and local tissue movement, that are preponderant near major blood vessels [3]. Some various strategies have been developed to reduce these effects but it remains some important difficulties, especially on long-TR datasets (typically TR$<$500 ms) where respiratory and particularly cardiac effects are aliased in the Nyquist bandwidth.

On the one hand, some existing methods using adaptive digital filtering [4] or retrospective correction [5][6] assume that the cardio-respiratory fluctuations were critically sampled and remained stationary which is not the case generally. On the other hand, spatial Independent Component Analysis proved its efficiency to identify patterns of structured noise in fMRI data [7]. The automatic selection of the corresponding components have been tested on short-TR datasets with frequency priors on cardio-repiratory activity [8]. Moreover, some other methods propose to regress out true physiology-related fmri signals (major vessels or CSF time-courses). We propose a method combining these two last approaches to remove structured-noise in fMRI. It consists of using true noise-related fMRI signals as priors to select noise-related independent components even with long-TR datasets.

2. CORSICA METHOD

2.1. sICA and noise reduction

Addressing the problem of blind source separation, spatial independent component analysis (sICA) allows to separate independent processes from a sequence. In our case, fMRI data is hypothesized to be the linear mixing of different brain processes whose spatial distributions are invariant over time and statistically independent. Even under such general hypotheses, sICA has proven to be able to decompose fMRI data into components that represent a specific brain phenomenon [7]. More precisely, sICA assumes the linear model:

$$\mathbf{X} = \mathbf{AS},$$

where $\mathbf{X}$ is the $T \times N$ matrix of fMRI time series with T time samples and N voxels; $\mathbf{S}$ is a $K \times N$ matrix of $K \leq T$ spatially independent sources (comprising N voxels each); $\mathbf{A}$ is the $T \times K$ matrix of the K corresponding time courses (comprising T samples each).

We used the Infomax algorithm [9] implemented in FMRLAB software[1] to perform sICA on the fMRI datasets, with Principal Component Analysis (PCA) as a preprocessing step in order to whiten data (without data dimension reduction, i.e. $K = N$). The spatial sources $\hat{\mathbf{S}} = (\hat{S}_i)_{i=1}^{K}$ were estimated by computing a mixing matrix $\mathbf{W}$ which represents a linear transformation of the data:

$$\hat{\mathbf{S}} = \mathbf{WX}.$$

Obviously, the efficiency of physiological noise reduction based on sICA depends on how accurately noise-related components can be selected. We then proposed a new method of selection that makes use of spatial priors related to the spatial distribution of cardio-respiratory effects in fMRI series (see part 2.2).

Then, after selecting this relevant subset $\hat{\mathbf{A}}_{noise}$ of noise-related independent components, it was straightforward to remove the structured noise from the data: these noise-related components were set

[1]http://www.sccn.usd.edu/fmrlab

to zero and the data were reconstructed from the remaining components $\hat{\mathbf{A}}_{int}$ (such that $\hat{\mathbf{A}} = \hat{\mathbf{A}}_{noise} \cup \hat{\mathbf{A}}_{int}$).

2.2. Noise-related components selection

The physiological signals were extracted from data in two specific regions of interest (ROIs) : the first comprising the first three ventricles to detect especially global and respiration-related movements and the second comprising the brainstem, the fourth ventricle and the basilar arteries to detect local cardiac activity. Because of the large spatial extent of these ROIs, we reduced further the number of characteristic signals by clustering the voxels of each mask into N_C clusters by using a conventional k-means algorithm, with distance d between two voxels function of the correlation between the time courses of the voxels [10]. The choice of the optimal number of classes N_C is discussed in the next part. We then defined for the two ROIs N_C signals characterizing the structured-noise by averaging the times courses in each cluster.

Then, a stepwise regression procedure was used to select among the K temporal components $\hat{\mathbf{A}} = \{\hat{A}_1, \ldots, \hat{A}_K\}$ obtained from sICA decomposition, the components whose time courses explained these N_C noise characteristic signals. Let $\mathbf{Y} = \{Y_1, \ldots, Y_{N_C}\}$ be the average time courses of the N_C selected regions, normalized to zero mean and unit variance. For each region element of $\mathbf{Y}$, we wished to select a subset of independent components explaining its characteristic signal Y_i. To do so, we used a stepwise regression procedure (stepwise forward-backward) [11]. For each signal Y_i, this iterative algorithm selected at each step a new independent component that was significantly partially correlated with Y_i (stepwise forward) and then removed the already selected components that were no longer significantly partially correlated with Y_i (stepwise backward). The procedure ended when no more significant component (according to the given statistical threshold) was found in stepwise forward. This procedure was repeated for each signal Y_i, finally yielding N_C subsets $(\mathbf{V}_i)_{i=1}^{N_C}$ of noise-related components.

For each ROI, we would remove from the data the major phenomenons that influenced (at various levels) the most clusters defined in this ROI. Then, the influence of each component in each ROI might be evaluated by the relative number of subsets $\mathbf{V}_i$ containing this component. This indicae, F_q is calculated for the two ROIs independently (because each ROI were built to not capture the same type of fluctuations) and the final value of F_q for each component was the maximum one. The components whose $F_q > F_q^{limit}$ were selected. Moreover, to prevent us from the Kmeans clustering variability, this indicae was calculated from N_R repetition of the selection procedure (Kmeans clustering and stepwise regression). The choice of the number of repetition N_R and the influence of the threshold F_q^{limit} was discussed hereafter.

3. CONTEXT OF VALIDATION

3.1. real datasets

EPI functional data were acquired on three right-handed volunteers with a 3T Bruker scanner in the fMRI center in Marseille (France) according to a protocol approved by the regional ethic committee. The subjects were scanned during three different conditions : during continuous rest consisting of remaining eyes closed, during continuous motor task consisted of performing a finger sequence with the left hand and during a blocked design motor task with the same task (the protocol was designed to test some hypothesis on the learning mechanisms and was not detailed here). For each subject, 7 long-TR datasets (1 rest, 4 continuous task and 2 blocked design task) and 3 short-TR datasets (1 rest, 1 continuous task and 1 blocked design task) were acquired. For long-TR datasets, 136 T_2^*-weighted volumes of 42 contiguous slices were recorded (the FOV was 192 mm with a 64×64 matrix size and a 3×3 mm in-plane voxel size, TR/TE = 2333/30 ms and $\alpha = 81^\circ$). For short-TR datasets, 950 T_2^*-weighted volumes of 2 groups of 3 contiguous 3-mm-thick slices, one group centered on the motor cortex and the other on the ventricles (the FOV was 192 mm with a 64×64 matrix size and a 3×3 mm in-plane voxel size, TR/TE = 333/30 ms and $\alpha = 40^\circ$). The heartbeat rhythm by plethysmography and the respiratory rhythm by using a respiratory belt were recorded during the acquisitions. The resulting raw data were corrected for slice-timing effects by using the SPM99 software, corrected for quadratic drifts by using linear regression and mean corrected.

3.2. References and validation

sICA was computed on the 21 long-TR datasets and the resulted components were visually inspected by two experts. The first 60 components of each dataset (the independent components were sorted in the decreasing order respect to the part of data variance explained) were classified into 4 groups : group 3 hold the components related to physiological fluctuations or movements exhibiting major activity in the ventricles or in the brainstem, group 2 hold the components related to the other types of artifacts, group 1 hold the components clearly related to functional activity and group 0 hold all other components. This classification was used as a reference to discuss on the influence of the parameters N_C, N_R of CORSICA in order to fix them.

Afterwards, we tested the CORSICA method with those fixed parameters on the short-TR datasets. sICA was computed on the 9 short-TR datasets . We used the cardio-repiratory monitored signals as reference to select physiology-related in order to compare these approach to CORSICA. The power spectra of the time courses of all K independent components were linearly regressed on the power spectra of the two physiological signals. An F-score was calculated to test the null hypothesis $H_0 : C_p = 0$. Each component for which the null hypothesis was rejected with $p < 0.001$ was considered to be related to physiology and included in group 3. Then, the first 60 components of each dataset, not classified in group 3, were visually inspected to identify the components clearly related to functional activity which were included in group 1. All other components are included in group 0.

4. RESULTS

We first applied the CORSICA method on long-TR datasets. The figure 1 showed the influence of N_C and N_R on the optimal sensitivity on the group 3 of the method (the sensitivity on the group g, $Sens_g$, is defined as the ratio between the number of components of the group g selected by CORSICA and the total number of components of the group g - the so-called optimal sensitivity is the value of $Sens_g$ for the lower value of F_q^{limit} as $Sens_1 = 0$). The results showed that for $N_C \geq 15$ and for $N_R \geq 3$, the selection was consistent on the three subjects and sensitive, and it was much more sensitive on the first 20 components (the one explaining the main part of the data variance) than on the first 60. Then, we fixed $N_C = 15$ and $N_R = 3$ (the processing time increase linearly

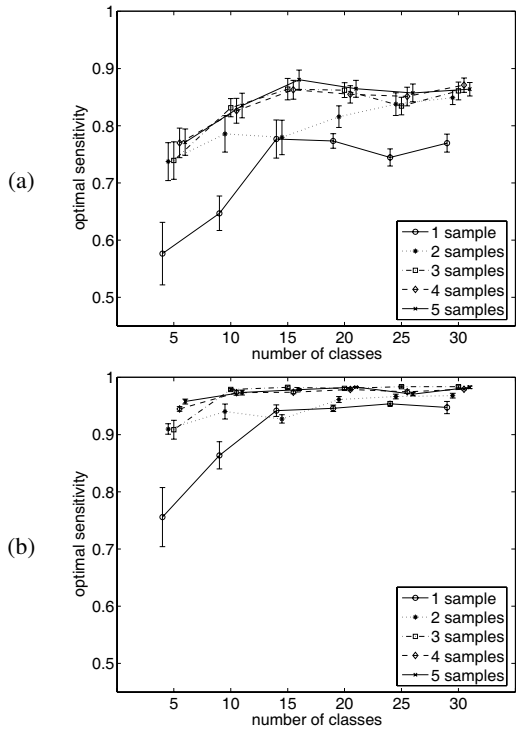

Fig. 1. *Long-TR data : Optimal value of Sen_3 function of N_C on the 60 first components (a) on the 20 first components (b)*

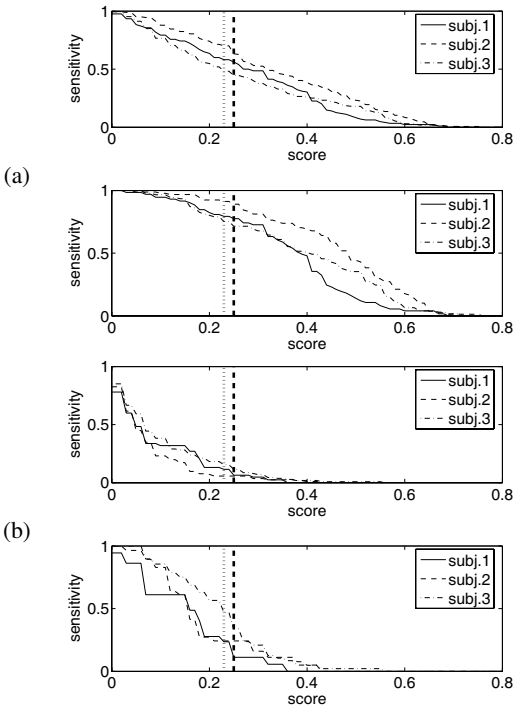

Fig. 2. *Long-TR data : (a) $Sens_3$ function of F_q^{lim} on the 60 first components (top) on the 20 first components (bottom); (b) $Sens_2$ function of F_q^{lim} on the 60 first components (top) on the 20 first components (bottom)*

with N_C and N_R) and we computed F_q for each component of each dataset. $Sens_3$ and $Sens_2$ were calculated for each value of F_q^{limit} (their mean values on each subject was shown in figure 2). The dotted vertical line is the lower value of F_q^{limit} as $Sens_1 > 0$ for at least one of the 21 datasets. It appeared that, for this value of F_q^{limit}, $Sens_3$ was comprised between $0,5$ and $0,75$ for the first 60 components and was comprised between $0,8$ and $0,95$ for only the 20 first ones. Moreover, it appeared that CORSICA was able to select some noise components of the group 2 which were not specific target of the method. Therefore, the distribution of the critical threshold F_q^{limit} chosen individually for each dataset had a mean of 0,09 (median = 0,08). For this "adapted" threshold, the sensitivity increased until 0,98 (see figure1). We then decided to take $F_q^{limit} = 0,25$ (dashed vertical line in figure 2) to test the full automatic method on the short-TR dataset.

The figure 3 showed that with the fixed set of parameters ($N_C = 15$, $N_R = 3$ and $F_q^{limit} = 0,25$), the CORSICA method, applied on short-TR datasets, was able to select a large majority of the physiology-related components. The table 1 showed the variance variation between the uncorrected data and corrected data in cerebro-spinal fluid (CSF), grey matter (GM) and white matter (WM). It appeared that, as expected, the correction was important in the CSF but also really efficient in the GM where the correction was necessary to capture cleaner functional signals. Moreover, with short-TR data we were able to calculate the power spectrum of the signals in the cardiac and respiratory frequency bandwidth before and after correction. The mean of the power spectrum calculated in the grey matter for subject 1 was plotted figure 4. The whole cardiac effect and the main part of the respiratory effect were corrected.

5. DISCUSSION

We proposed a method of structured noise correction, CORSICA, based on the ability of sICA to identifying patterns of structured noise in fMRI and on the use of time-courses of brain regions specifically influenced by structured noise. On the one hand, the use of this kind of a priori allows the method to be applied not only on short-TR datasets (where cardio-respiratory rhythms are critically sampled) but also on long-TR data. On the other hand, it allows not to make unrealistic assumptions on signal stationarity and frequency localization used in many others methods of noise correction in fMRI. The method was able to calculate a score for each independent components which allowed to discriminate the physiology-related components from the components related to functional activity. The choice of the threshold appeared to be critical but it was possible to propose a conservative threshold leading to the correction of the main effects in a full automatic way (see results in short-TR datasets). Therefore, the noise correction could be individually improve if the threshold is adapted, leading to a semi-automatic correction.

However, our method of noise reduction based on the selection of noise-related components are obviously narrowly linked to the ability of sICA to separate physiology-related phenomena from the other brain processes. If physiology-related signals and neural-activity-related signals remained mixed into several compo-

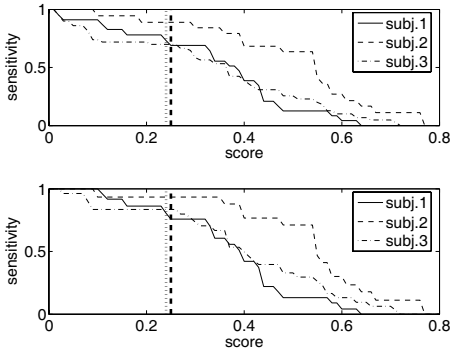

Fig. 3. *Short-TR data : (a) $Sens_3$ function of F_q^{lim} on the 60 first components (top) on the 20 first components (bottom)*

		csf	gm	wm
subj.1	block	0,18	0,14	0,14
	continu	0,13	0,09	0,09
	rest	0,12	0,10	0,10
subj.2	block	0,29	0,17	0,14
	continu	0,16	0,09	0,08
	rest	0,23	0,12	0,10
subj.3	block	0,21	0,14	0,12
	continu	0,22	0,13	0,11
	rest	0,19	0,12	0,11
mean		**0,19**	**0,12**	**0,11**

Table 1. *Short-TR data : Normalized variations of the variance (in %) in cerebro-spinal fluid (csf), grey matter (gm) and white matter (wm).*

nents, the method of selection we proposed might suppress a part of signal of interest. So, to improve the method, it seemed to be important to control the independent components separation, eventually by incorporating in the sICA model some prior information on spatio-temporal characteristics of cardio-respiratory effects we would identify and remove.

6. REFERENCES

[1] D. Raj, A. W. Anderson, and J. C. Gore, "Respiratory effects in human functional magnetic resonance imaging due to bulk susceptibility changes," *Physics in Medicine and Biology*, vol. 46, pp. 3331–3340, 2001.

[2] C. Windischberger, H. Langenberger, T. Sycha, E. M. Tschernko, G. Fuchsjger-Mayerl, L. Schmetterer, and E. Moser, "On the origin of respiratory artifacts in BOLD-EPI of human brain," *Magnetic Resonance Imaging*, vol. 20, pp. 575–582, 2002.

[3] M. S. Dagli, J. E. Ingeholm, and J. V. Haxby, "Localization of cardiac-induced signal change in fMRI," *Physics in Medicine and Biology*, vol. 9, pp. 407–415, 1999.

[4] B. Biswal, E. A. DeYoe, and J. S. Hyde, "Reduction of physiological fluctuations in fMRI using digital filters," *Magnetic Resonance in Medicine*, vol. 35, pp. 107–113, 1996.

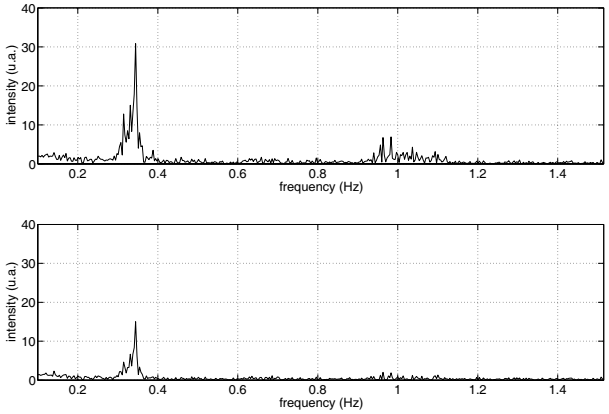

Fig. 4. *Short-TR data : Mean of the power spectrum of the signals in grey matter for subject 1*

[5] X. Hu, T. H. Le, T. Parrish, and P.Erhard, "Retrospective estimation and correction of physiological fluctuations in functional MRI," *Magnetic Resonance in Medicine*, vol. 34, pp. 201–212, 1995.

[6] G. H. Glover, T. Q. Li, and D. Ress, "Image-based method for retrospective correction of physiological motion effects in fMRI: RETROICOR," *Magnetic Resonance in Medicine*, vol. 44, pp. 162–167, 2000.

[7] M. J. McKeown, S. Makeig, and G. G. Brown, "Analysis of fMRI data by blind separation into independent spatial components," *Human Brain Mapping*, vol. 6, pp. 160–188, 1998.

[8] C. G. Thomas, R. A. Harshman, and R. S. Menon, "Noise reduction in BOLD-based fMRI using component analysis," *NeuroImage*, vol. 17, pp. 1521–1537, 2002.

[9] A. J. Bell and T. J. Sejnowski, "An information maximization approach to blind separation and blind deconvolution," *Neural Computation*, vol. 7, pp. 1129–1159, 1995.

[10] J. A. Hartigan, *Clustering Algorithms*, John Wiley and Sons Inc, New-York, 1975.

[11] N. R. Draper and H. Smith, *Applied Regression Analysis*, John Wiley and Sons Inc, New-York, 2001.